 doi: 10.1111/j.1471-4159.2007.05153.x

Cell type-specific subunit composition of G protein-gated potassium channels in the cerebellum

Carolina Aguado,* José Colón,† Francisco Ciruela,‡ Falk Schlaudraff,§,¶ Maria José Cabañero,* Cydne Perry,† Masahiko Watanabe,** Birgit Liss,§,¶ Kevin Wickman† and Rafael Luján*

*Departamento de Ciencias Médicas, Facultad de Medicina, Universidad de Castilla-La Mancha, Campus Biosanitario, Albacete, Spain

†Department of Pharmacology, University of Minnesota, Minneapolis, Minnesota, USA

‡Departament de Bioquímica i Biologia Molecular, Universitat de Barcelona, Barcelona, Spain

§Department for Physiology, Philipps University Marburg, Marburg, Germany

¶Departement for General Physiology, University Ulm, Ulm, Germany

**Department of Anatomy, Hokkaido University School of Medicine, Sapporo, Japan

Abstract

G protein-gated inwardly rectifying potassium (GIRK/Kir3) channels regulate cellular excitability and neurotransmission. In this study, we used biochemical and morphological techniques to analyze the cellular and subcellular distributions of GIRK channel subunits, as well as their interactions, in the mouse cerebellum. We found that GIRK1, GIRK2, and GIRK3 subunits co-precipitated with one another in the cerebellum and that GIRK subunit ablation was correlated with reduced expression levels of residual subunits. Using quantitative RT-PCR and immunohistochemical approaches, we found that GIRK subunits exhibit overlapping but distinct expression patterns in various cerebellar neuron subtypes. GIRK1 and GIRK2 exhibited the most widespread and robust labeling in the cerebellum, with labeling particularly prominent in granule cells. A high degree of molecular diversity in the cerebellar GIRK channel repertoire is suggested by labeling seen in less abundant neuron populations, including Purkinje neurons (GIRK1/GIRK2/GIRK3), basket cells (GIRK1/GIRK3), Golgi cells (GIRK2/GIRK4), stellate cells (GIRK3), and unipolar brush cells (GIRK2/GIRK3). Double-labeling immunofluorescence and electron microscopies showed that GIRK subunits were mainly found at post-synaptic sites. Altogether, our data support the existence of rich GIRK molecular and cellular diversity, and provide a necessary framework for functional studies aimed at delineating the contribution of GIRK channels to synaptic inhibition in the cerebellum.

Keywords: GIRK, heteromultimerization, immunohistochemistry, Kir3, potassium channel, subunit composition.

J. Neurochem. (2007) 10.1111/j.1471-4159.2007.05153.x

Neuronal G protein-gated inwardly rectifying K^+ (GIRK/Kir3) channels mediate the slow post-synaptic inhibitory effect of numerous neurotransmitters and related drugs of abuse (North 1989; Lüscher *et al.* 1997). Four mammalian GIRK subunit genes (GIRK1–4) have been identified, and alternative splicing of the GIRK2 gene yields multiple distinct protein products (Wei *et al.* 1998). These observations, as well as evidence for expression of all four subunits in the CNS (Karschin *et al.* 1996; Liao *et al.* 1996; Murer *et al.* 1997), have fueled speculation that neuronal GIRK channels exhibit significant molecular and functional diversity.

G protein-gated inwardly rectifying K^+ channels subunits combine to form homo- and heterotetrameric channels in expression systems and *in vivo* (e.g. Kobayashi *et al.* 1995; Krapivinsky *et al.* 1995a,b; Lesage *et al.* 1995). While random tetrameric assembly of four distinct subunits would generate a heterogeneous population of neuronal GIRK channels, several observations suggest that the molecular

Received October 11, 2007; revised manuscript received November 17, 2007; accepted November 20, 2007.

Address correspondence and reprint requests to Dr Rafael Luján, Department Ciencias Médicas, Facultad de Medicina, Universidad de Castilla-La Mancha, Campus Biosanitario, C/Almansa 14, Albacete 02006, Spain. E-mail: Rafael.Lujan@uclm.es

Abbreviations used: DTT, dithiothreitol; EGFP, enhanced green fluorescent protein; ER, endoplasmic reticulum; GAD, glutamic acid decarboxylase; GFAP, glial fibrilary acidic protein; GIRK, G protein-gated inwardly rectifying K^+ channel; GST, glutathione *S*-transferase; KO, knockout; LMD, UV-laser microdissection; PB, phosphate buffer; PC, Purkinje cell; RIPA, radioimmuno precipitation assay; SDS, sodium dodecyl sulfate; vGluT, vesicular glutamate transporter; WT, wild-type.

diversity of neuronal GIRK channels is limited. First, GIRK4 expression is restricted to a small number of neuron populations (Wickman *et al.* 2000). Second, GIRK1 contains an endoplasmic reticulum (ER) retention signal and requires co-expression with another GIRK subunit to achieve membrane distribution (Krapivinsky *et al.* 1995a; Hedin *et al.* 1996; Kennedy *et al.* 1996; Ma *et al.* 2002). Third, GIRK3 has been proposed to function in a channel-trafficking capacity, directing functional GIRK channels toward lyzosomal degradation (Ma *et al.* 2002). Thus, the neuronal GIRK channel population is often considered to consist primarily, if not exclusively, of GIRK1/GIRK2 heteromultimers or GIRK2 homomultimers.

Although neuronal GIRK channels may consist primarily of GIRK1 and/or GIRK2, compelling data argue that other subunit combinations are relevant and exhibit unique functional properties. For example, GIRK2/GIRK3 heteromeric complexes, which exhibit a reduced sensitivity to Gβγ and have been isolated from the mouse brain (Jelacic *et al.* 2000), may carry the metabotropic GABA receptor-dependent GIRK current in dopamine neurons of the ventral tegmental area (Cruz *et al.* 2004). Recent ultrastructural data from the hippocampus and spinal cord has shown that GIRK2, but not GIRK1, is present within the post-synaptic specialization (Koyrakh *et al.* 2005; Marker *et al.* 2005). Furthermore, membrane fractionation has indicated that GIRK2 and GIRK3 are present in distinct membrane microdomains in the hippocampus (Koyrakh *et al.* 2005). Thus, subunit composition may influence the subcellular distribution, and consequently the functional relevance, of neuronal GIRK channels.

While the functional implications of GIRK channel subunit composition *in vivo* remain largely unknown, it seems reasonable to speculate that subunit composition confers unique functionality to GIRK channels and host neurons. In this regard, the cerebellum is an ideal structure for examining diversity within the neuronal GIRK channel repertoire. Moreover, *in situ* hybridization suggests that GIRK1, GIRK2, and GIRK3 mRNAs are present in the cerebellum (Karschin *et al.* 1996; Liao *et al.* 1996). Accordingly, we used molecular and morphological approaches to identify the subunit composition of GIRK channels in the various neuron populations in the cerebellum. We report an unexpectedly diverse array of GIRK channel subtypes distributed in a cell type-specific manner.

Materials and methods

Animals

All animal use was approved by the Institutional Animal Care and Use Committee of the University of Castilla-La Mancha and followed Spanish and European Union regulations. Efforts were made to minimize the pain and discomfort of the animals throughout the study. The generation of GIRK knockout (KO) mice was described previously (Signorini *et al.* 1997; Wickman *et al.* 1998; Bettahi *et al.* 2002; Torrecilla *et al.* 2002). Age- and sex-matched wild-type (WT) mice were obtained from Charles River Laboratories (Barcelona, Spain) and they were housed on a 12 h light/dark cycle, with food and water available *ad libitum*. The Tg(Kcnj5-EGFP)49Gsat mouse expressing enhanced green fluorescent protein (EGFP) under the control of the Girk4/Kcnj5 promoter was obtained from the Mutant Mouse Regional Resource Center, generated as part of the GENSAT BAC transgenic project (NINDS contract #NO1-NS-0-2331).

Antibodies

A complete list of the primary and secondary antibodies, including their source, dilution and combined use, used for this study is given in Table 1. All secondary antibodies were purchased from commercial sources (Table 1). We also developed polyclonal antibodies to the mouse GIRK1–3 (Kir3.1–3.3) against the C-terminal sequences of GIRK1 (33 amino acid residues, accession number P35562), GIRK2 (32 aa, P48542), and GIRK3 (22 aa, Q63511) (Fig. 1a). The 32 aa C-terminal domain used to generate the GIRK2 antibodies corresponds to residues 390–421 of GIRK2C and 370–401 of GIRK2D and partially overlaps with residues 390–414 of GIRK2A (Fig. 1a, underline), but is not represented in the GIRK2B isoform.

Antigens were prepared as glutathione *S*-transferase (GST) fusion proteins, as reported previously (Nakamura *et al.* 2004). GST fusion proteins were injected into female rabbits and guinea pigs at intervals of 2 weeks. A week after the sixth injection, immunoglobulins specific to GIRK1–3 were purified from the antisera using affinity media coupled with GST-free polypeptides. Using similar approaches, we also attempted to generate antibodies against GIRK4. Unfortunately, we failed to obtain antisera exhibiting specific labeling for GIRK4 as assessed by parallel immunohistochemical analysis of WT and GIRK4 KO brain tissue (data not shown). Thus, we used a BAC transgenic line that expresses EGFP under the control of the *Girk4* promoter [Tg(Kcnj5-EGFP)49Gsat, obtained from Mutant Mouse Regional Resource Center, University of California, Davis, CA, USA] to determine the cerebellar distribution of the GIRK4 subunit.

Immunoblotting and immunoprecipitation

The specificity of GIRK antibodies and expression of GIRK subunits were analyzed by immunoblotting analysis using cerebellar homogenates. Cerebella from adult WT and GIRK KO mice were extracted and homogenized in 2 mL of buffer containing (in mmol/L) 25 Tris, pH 7.5, 150 NaCl, 5 EDTA, pH 8.0, and 1 dithiothreitol (DTT) and a protease inhibitor mixture containing 0.35 μg/mL phenylmethylsulfonyl fluoride, 1.7 μg/mL aprotinin, 0.7 μg/mL pepstatin, and 10 μg/mL leupeptin. Samples were centrifuged at low speed (2200 *g*) to eliminate nuclei and large debris, and the crude membrane fraction was then pelleted by centrifugation at 200 000 *g* for 30 min. Pellets were resuspended in 1 mL of a 2% sodium dodecyl sulfate (SDS) solution containing 1 mmol/L DTT and the protease inhibitor mixture. Samples were centrifuged for 5 min at 500 *g* to remove insoluble contents. Protein concentration was measured using the Lowry assay (Sigma Aldrich, St Louis MO, USA). Immunoblotting was performed as described previously (Bettahi *et al.* 2002; Marker *et al.* 2002). Densitometry was performed using ImageQuant software (Molecular Dynamics,

Table 1 Summary of antibodies, their dilutions and sources, and figures employed each antibody

Primary Ab	Species	Dilution	Secondary Ab	Dilution	Figure	Source of primary Ab	Characterization
GIRK1	Rabbit	1 : 300	Gt anti-Rb HRP (WB)[a]	1 : 30 000	Fig. 3	Alomone, Israel	Koyrakh *et al.* 2005;
GIRK1	Rabbit	1 : 400	Gt anti-Rb HRP (WB)[a]	1 : 30 000	Fig. 1	Professor M. Watanabe	This article, Fig. 1
			Gt anti-Rb biotin (IP)[a]	1 : 100	Fig. 2		
			Gt anti-Rb biotin (LM)[b]	1 : 100	Figs 1, 4, 7, and 8		
			Alexa®488 Gt anti-Rb (IF)[d]	1 : 1000	Fig. 5		
			1.4 nm-gold Gt anti-Rb (EM)[e]	1 : 100	Figs 6 and 7		
GIRK1	Guinea pig	1 : 400	Gt anti-Gp HRP (WB)[c]	1 : 30 000	Fig. 1	Professor M. Watanabe	This article
			Gt anti-Gp biotin (LM)[b]	1 : 100	Fig. 1		
			Alexa®488 Gt anti-Gp (IF)[f]	1 : 500	Fig. 5		
GIRK2	Rabbit	1 : 500	Gt anti-Rb HRP (WB)[a]	1 : 30 000	Fig. 3	Alomone, Israel	Koyrakh *et al.* 2005;
GIRK2	Rabbit	1 : 800	Gt anti-Gp HRP (WB)[a]	1 : 30 000	Fig. 1	Professor M. Watanabe	This article, Fig. 1
			Gt anti-Rb biotin (LM)[b]	1 : 100	Fig. 1		
GIRK2	Guinea pig	1 : 800	Gt anti-Gp HRP (WB)[c]	1 : 30 000	Fig. 1	Professor M. Watanabe	This article, Fig. 1
			Gt anti-Rb biotin (IP)[c]	1 : 100	Fig. 2		
			Gt anti-Gp biotin (LM)[b]	1 : 100	Figs 1, 4, 7 and 8		
			Alexa®488 Gt anti-Gp (IF)[d]	1 : 1000	Figs 5 and 8		
			Cy3 Gt anti-Gp (IF)[f]	1 : 500	Figs 5 and 8		
			1.4 nm-gold Gt anti-Gp (EM)[e]	1 : 100	Figs 6 and 7		
GIRK3	Rabbit	1 : 500	Gt anti-Rb HRP (WB)[a]	1 : 30 000	Fig. 3	Alomone, Israel	Koyrakh *et al.* 2005;
GIRK3	Rabbit	1 : 400	Gt anti-Rb HRP (WB)[a]	1 : 30 000	Fig. 1	Professor M. Watanabe	This article, Fig. 1
			Gt anti-Rb biotin (IP)[a]	1 : 100	Fig. 2		
			Gt anti-Rb biotin (LM)[b]	1 : 100	Figs 1, 4, 7, and 8		
			Cy3 Gt anti-Gp (IF)[f]	1 : 500	Fig. 8		
			1.4 nm-gold Gt anti-Rb (EM)[e]	1 : 100	Fig. 6 and 7		
VGAT	Rabbit	1 : 500	Alexa®488 Gt anti-Rb (IF)[d]	1 : 1000	Figs 8 and S1	Professor M. Watanabe	Fukudome *et al.* 2004;
mGlu2/3	Rabbit	1 : 400	Alexa®488 Gt anti-Rb (IF)[d]	1 : 1000	Fig. 8	Chemicon, Temecula, CA, USA	Not available (AB1553)

WB, western blots; IP, co-immunoprecipitation; LM, light microscopy immunoperoxidase; IF, immunofluorescence; EM, electron microscopy; Gt, goat; Rb, rabbit; M, mouse; Gp, guinea pig. [a]Pierce Biotech, Rockford, USA; [b]Vector Laboratories, Burlingame, CA, USA; [c]Southern Biotech, Birmingham, AL, USA; [d]Molecular Probes, Leiden, Holland; [e]Nanoprobes Inc., Stony Brook, NY, USA; [f]Jackson Laboratories, Baltimore, PA, USA.

Sunnyvale, CA, USA). For analysis of GIRK subunit levels in the cerebellum, the density of the appropriate region in the lane loaded with corresponding KO samples relevant to the target antibody was taken as the background (density value = 0). For each of the three panels of WT and GIRK KO mice, three blots for each GIRK subunit were run, and signal intensities were averaged to obtain a single data point. All data points were normalized to the mean signal intensity calculated from the WT samples.

For immunoprecipitation, membranes from the cerebellum were obtained as described previously (Ciruela *et al.* 2001; Burgueno *et al.* 2003) and solubilized in ice-cold radioimmuno precipitation assay (RIPA) buffer (Pierce, Rockford, IL, USA) (50 mmol/L Tris–HCl, pH 7.4, containing 1% (v/v) Triton X-100, 0.2% SDS, 0.5% deoxycholate, 100 mmol/L NaCl, and 1 mmol/L EDTA) for 30 min on ice. The solubilized preparation was then centrifuged at 16 000 *g* for 30 min. The supernatant (1 mg/mL) was processed for immunoprecipitation, each step of which was conducted with constant rotation at 0–4°C. The supernatant was incubated overnight with the indicated antibody. Then 40 μL of a suspension of anti-rabbit IgG beads (TrueBlot; eBioscience, San Diego, CA, USA) was added and the mixture was incubated for 2 h with constant rotation at 4°C. The beads were washed twice with ice-cold RIPA buffer, twice with ice-cold RIPA buffer containing 0.1% Triton X-100, 0.02% SDS, 0.05% deoxycholate and once with phosphate-buffered saline and aspirated to dryness with a 28-gauge needle. Subsequently, 30 μL of SDS–polyacrylamide gel electrophoresis sample buffer (8 mol/L urea, 2% SDS, 100 mmol/L DTT, and 375 mmol/L Tris, pH 6.8) was added to each sample. Immunocomplexes were dissociated by heating to 37°C for 2 h, resolved by SDS-polyacrylamide gel electrophoresis in 10% gels, and immunoblotted as described above.

UV-laser microdissection and quantitative RT-PCR

Male C57BL/6 mice (3- to 5-week old) were used for contact-free UV-laser-microdissection (LMD6000; Leica Microsystems, Wetzlar, Germany) and collection of individual cells (20–25 cells each pool) of distinct cerebellar cell types [Purkinje cells (PCs), basket cells, stellate cells, and granule cells] from coronal brain-cryosections, and subsequent GIRK1–4 mRNA expression-profiling. LMD, cDNA-synthesis, and cDNA purification as well as qualitative and quantitative RT-PCR (Applied Biosystems 7900HT thermocycler,

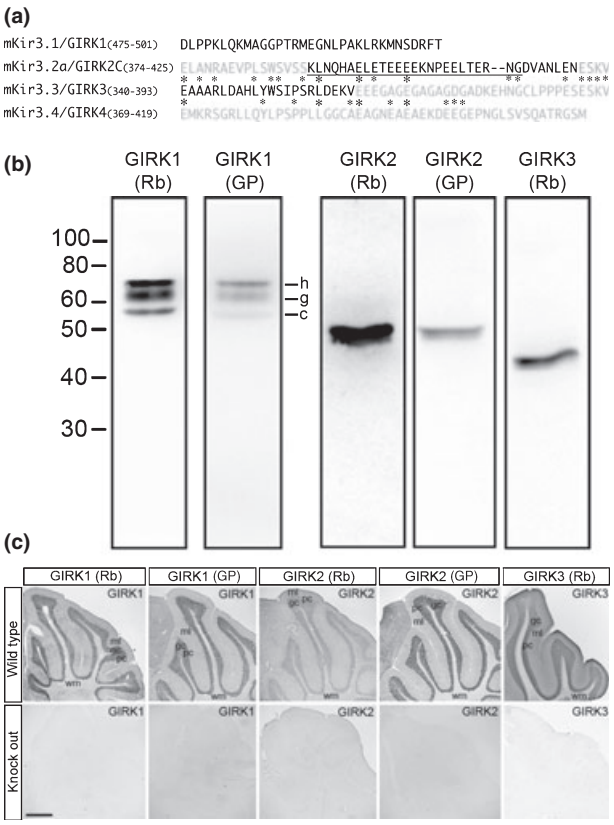

Fig. 1 Production and specificity of GIRK1, GIRK2, and GIRK3 antibodies in the cerebellum using immunoblotting and immunohistochemical techniques. (a) Amino acid sequence alignment of antigenic regions used for GIRK1, GIRK2, and GIRK3 antibody production. Asterisks indicate amino acid residues identical between GIRK2 (GenBank accession number P48542) and GIRK3 (Q63511). An underline indicates antigen sequence of GIRK2C that overlaps with GIRK2A isoform. (b) By immunoblot, rabbit (Rb), and guinea pig (GP) GIRK1 antibodies recognize three protein bands of ~70, ~65 and ~55 kDa, corresponding to heavily glycosylated (h), core-glycosylated (g), and unglycosylated (c) versions of the GIRK1 protein, respectively; rabbit (Rb) and guinea pig (GP) GIRK2 antibodies recognize a doublet at ~49 kDa, with the upper band showing stronger labeling, similar to previous observations (Koyrakh *et al.* 2005); and rabbit (Rb) GIRK3 antibodies recognize a protein band of ~45 kDa. (c) Immunohistochemistry for the different GIRK subunits in the cerebellum of wild-type mice. No staining was found in cerebellar sections from the corresponding GIRK KO mice. Scale bar: 0.5 mm.

Foster City, CA, USA) were carried out essentially as described (Liss 2002; Liss *et al.* 2005).

RT-PCRs were performed in a final volume of 20 µL utilizing 2x QuantiTect SYBR-Green Mix (Qiagen, Hilden, Germany). Multiplex-nested PCR-primer-sequences for mouse calbindin-$_{d28k}$, glial fibrilary acidic protein (GFAP), and glutamic acid decarboxylase (GAD)65/67 as described (Liss *et al.* 1999), for vesicular glutamate transporter (vGluT1; accession number NM-08085) primer-sequences were 1037-TTGCGCAGTCGTCACATAAT (F1), 1932-GAGGTTGAACTGTCCCTCCA (R1), 1649-GCAGTTTCCAGG-ACTTCCAC (F2), and 1855-ACTTTCAGGGGAGTCTGGGTA (R2). Primers for SYBR-green quantitative RT-PCR were selected using the Oligo 6.0 primer analysis software (Medprobe, Oslo, Norway). Primer sequences for GIRK1 (accession number NM-008426.1) 657-GAGGGACGGAAAACTCACTCT (F), TCAGGT-GTCTGCCGAGATT-765 (R); for GIRK2 (accession number NM-010606.2) (GIRK2A), NM-001025585.2 (GIRK2B), NM-001028854.2 (GIRK2C), 432-CGTGGAGTGAATTATTGAATCT (F), GTCATTTCTTCTTTGTGCTTTT-534 (R); for GIRK3 (accession number NM-008429.2) 34-CAGAGGGAACCTAGGGTACTG (F), TTCCTAGGCTTTCAGGGTC-151 (R) and for GIRK4 (accession number NM-010605.3) 95-AAGTTAGCCCCAAGGGTTCG (F), CTGCCATGCTCCCAAGTACAC-196 (R).

Immunohistochemical analysis

Mice were anesthetized by intraperitoneal injection of ketamine (0.1 mL /kg b.w.) and xylazine (0.1 mL /kg b.w.) and perfused with 4% *p*-formaldehyde and 15% (v/v) saturated picric acid made up in 0.1 mol/L phosphate buffer (PB; pH 7.4). After perfusion, brains were dissected and post-fixed in the same fixative at 4°C for 2 h. Coronal (60 µm) sections were then cut on a Vibratome (Leica V1000) and collected in 0.1 mol/L PB. The sections were then processed further either for immunoperoxidase reaction or for double-immunofluorescence procedures as described previously (Luján *et al.* 1996; López-Bendito *et al.* 2002).

Electron microscopic analysis

Animals were perfused with 4% *p*-formaldehyde, 0.05% glutaraldehyde, and 15% (v/v) saturated picric acid made up in 0.1 mol/L PB (pH 7.4). Cerebellar sections were treated for electron microscopy immunolabeling as described (Luján *et al.* 1996; López-Bendito *et al.* 2002). Briefly, for pre-embedding immunogold labeling, brain sections (50–70 µm) were cut on a Vibratome and processed for immunohistochemical detection of GIRK1, GIRK2, and GIRK3 at a final protein concentration of 1–2 µg/mL using silver-enhanced immunogold techniques. Ultrastructural analyses were performed in a Jeol-1010 electron microscope (Jeol, Tokyo, Japan).

Controls

To test method specificity in the procedures for both light and electron microscopy, antisera against GIRK1, GIRK2, and GIRK3 were tested on brain slices of mice lacking the respective GIRK channel subunit. All other primary antibodies were either omitted or replaced with 5% (v/v) normal serum of the species of the primary antibody. Under these conditions, no selective labeling was observed. When double labeling for confocal microscopy was carried out, some sections were always incubated with only one primary antibody and the full complement of secondary antibodies to test for any cross-reactivity. Other sections were incubated with two primary antibodies and one secondary antibody, followed by the full sequence of signal detection. No cross-labeling was detected that would adversely impact the results.

Results

Antibody specificity

To analyze the expression and precise cellular and subcellular localization of GIRK1, GIRK2, and GIRK3 subunits in the

cerebellum, as well as their co-expression in specific cerebellar cell types, we produced polyclonal antibodies against the C-terminal sequences of mouse GIRK1, GIRK2, and GIRK3 subunits (Fig. 1a). Although the GIRK2 antibody is predicted to recognize the GIRK2A, GIRK2C, and GIRK2D splice isoforms (Inanobe *et al.* 1999a,b; Ma *et al.* 2002), in the interest of simplicity, we will refer to labeling revealed by this antibody as reflecting interactions with GIRK2. The antibodies were used first in immunoblotting experiments involving cerebellar extracts from the adult mice. The custom-derived GIRK1 antibodies produced in rabbit and guinea pig recognized three protein bands at ~70, ~65, and ~55 (Fig. 1b), which appeared to correspond to heavily glycosylated (h), core-glycosylated (g), and unglycosylated (core; c) versions of GIRK1 protein, respectively (Krapivinsky *et al.* 1995a; Kennedy *et al.* 1996). Consistent with previous studies and predicted molecular weights, GIRK2 antibodies produced in rabbit and guinea pig recognized a doublet at ~49 kDa, with the upper band showing stronger labeling, and the rabbit GIRK3 polyclonal antibody recognized a protein band at ~45 kDa (Fig. 1b).

We next proceeded to examine the regional expression of the GIRK subunits in the mouse cerebellum using immunohistochemical techniques and sagittal brain sections. In contrast to the robust and specific staining observed in WT mice with these antibodies, no staining was found in brain sections from the corresponding GIRK KO mice (Fig. 1c). These data confirm the specificity of the GIRK1, GIRK2, and GIRK3 antibodies in immunohistochemical approaches.

Physical association of GIRK subunits in cerebellar membranes

To determine whether GIRK1, GIRK2, and GIRK3 subunits form heteromeric complexes in the cerebellum, co-immunoprecipitation experiments were carried out using solubilized cerebellar membranes. All the antibodies tested were capable of immunoprecipitating the target subunit, as judged by the size of immunoprecipitated bands seen in subsequent immunoblotting (Fig. 2; GIRK1, lane 2 of top panel; GIRK2, lane 3 of middle panel; GIRK3, lane 4 of bottom panel). Furthermore, the GIRK1 antibody co-immunoprecipitated both GIRK2 and GIRK3 subunits (Fig. 2, top panel, lanes 3 and 4), the GIRK2 antibody co-immunoprecipitated GIRK1 and GIRK3 subunits (middle panel, lanes 2 and 4), and the GIRK3 antibody co-immunoprecipitated both GIRK1 and GIRK2 subunits (bottom panel, lanes 2 and 3). These observations suggest that the three neuronal GIRK subunits likely interact with one another in the cerebellum.

GIRK subunits are down-regulated in the cerebellum of GIRK KO mice

Given the co-precipitations observed for three neuronal GIRK subunits in cerebellar membrane extracts, one might predict that the loss of a given subunit would affect the

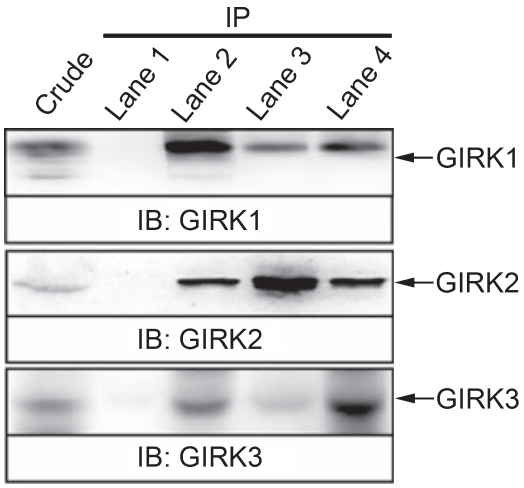

Fig. 2 Co-immunoprecipitation of GIRK channel subunits in the cerebellum. Membranes from cerebellum were solubilized and processed for immunoprecipitation using rabbit anti-FLAG polyclonal antibody as a control IgG (2 μg/mL; lane 1), rabbit anti-GIRK1 polyclonal antibody (1 μg/mL; lane 2), rabbit anti-GIRK2 polyclonal antibody (1 μg/mL; lane 3), or rabbit anti-GIRK3 polyclonal antibody (1 μg/mL; lane 3). Solubilized membranes (Crude) and immunoprecipitates (IP) were analyzed by SDS–polyacrylamide gel electrophoresis (20 μg of membrane proteins was always loaded) and immunoblotted using rabbit anti-GIRK1 polyclonal antibody (1/1000), rabbit anti-GIRK2 polyclonal antibody (1 : 1000) or rabbit anti-GIRK3 polyclonal antibody (1 : 1000). A HRP-conjugated anti-rabbit IgG TrueBlot™ (1 : 1000) was used as a secondary antibody in order to avoid IgG cross-reactivity. The immunoreactive bands were visualized by chemiluminescence.

expression and/or turnover of other subunits. We addressed this issue first in quantitative immunoblotting experiments involving GIRK KO mice (Fig. 3). We found that GIRK2 and GIRK3 subunits were reduced by 23 ± 1% ($p < 0.05$) and 69 ± 2% ($p < 0.01$), respectively, in the GIRK1 KO cerebellum (Fig. 3b). Similarly, the heavily glycosylated form of GIRK1 subunit was reduced by 49 ± 2% ($p < 0.01$) in GIRK2 KO cerebellum and 44 ± 3% ($p < 0.01$) in GIRK3 KO cerebellum. In GIRK2/GIRK3 double KO cerebellum, the heavily glycosylated form of GIRK1 subunit was reduced by 79 ± 3% ($p < 0.01$). Thus, the ablation of a given GIRK subunit correlates with diminished cerebellar content of the residual subunits, further supporting the contention that GIRK subunits likely co-assembled to form heteromeric GIRK channels in the cerebellum, similarly to our observations in the hippocampus (Koyrakh *et al.* 2005). Given that the mature glycosylation of GIRK1 subunit occurs as a consequence of heteromeric channel assembly and in parallel with its plasma membrane distribution (Krapivinsky *et al.* 1995a; Kennedy *et al.* 1999), the dramatic reduction noted in the GIRK2/GIRK3 double KO cerebellum argues that GIRK1 forms functional channels primarily with GIRK2 and GIRK3 subunits in the cerebellum.

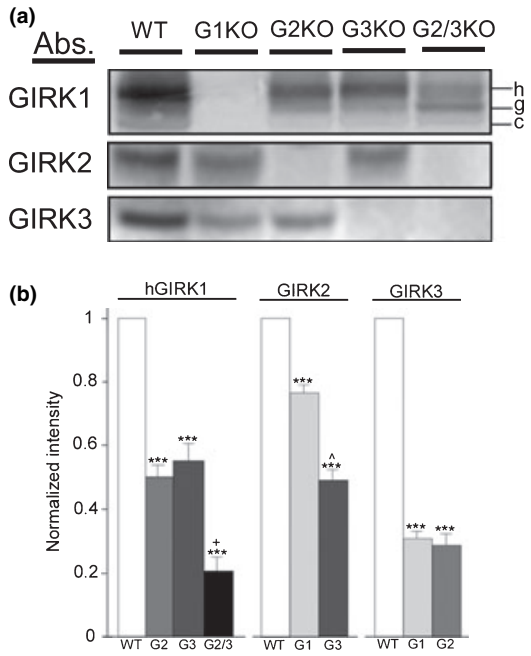

Fig. 3 Impact of GIRK subunit ablation on the expression of GIRK subunits in the cerebellum. (a) Representative immunoblots of cerebellar membrane protein samples from WT, GIRK1 (G1), GIRK2 (G2), GIRK3 (G3), and GIRK2/GIRK3 (G2/3) KO mice. For all the different blots, 20 μg of membrane protein was loaded. Blots were probed with antibodies (Abs) for GIRK1, GIRK2, and GIRK3. GIRK1 immunoreactivity was again visualized as three bands. Reduction in the level of the heavily glycosylated (h) GIRK1 species was correlated with the absence of GIRK2 and GIRK3, respectively. The levels of GIRK2 and GIRK3 were also lower in samples from KO mice. (b) Densitometric analysis of the impact of GIRK subunit ablation on residual GIRK protein levels in the cerebellum. Cerebellar protein samples were obtained from three separate and complete panels of WT and GIRK KO mice, and the levels of GIRK1 (heavily glycosylated form, h-GIRK1), GIRK2 and GIRK3 were determined. $^{***}p < 0.001$ compared with WT; $^{+}p < 0.01$ GIRK2/GIRK3 KO compared with GIRK2 KO and GIRK3 KO; $^{\wedge}p < 0.001$ GIRK3 KO compared with GIRK1 KO.

We also noted reduction of GIRK subunit labeling in immunohistochemical experiments involving WT and GIRK KO cerebella (Fig 4). Consistent with the quantitative immunoblotting data, GIRK1 immunolabeling was affected by the loss of either GIRK2 (Fig. 4c) or GIRK3 (Fig. 4d), and dramatically reduced in sections from GIRK2/GIRK3 double KO mice (Fig. 4e); in these sections, GIRK1 immunoreactivity was confined to cell bodies. GIRK2 immunolabeling was also found to be less intense in sections from GIRK1 KO mice (Fig. 4i) and GIRK3 KO mice (Fig. 4j), and absent in sections from GIRK2/GIRK3 double KO mice (Fig. 4k). Similarly, immunoreactivity for GIRK3 was significantly reduced in sections from GIRK1 KO mice (Fig. 4o) and GIRK2 KO mice (Fig. 4p), and missing in the GIRK2/GIRK3 double KO mice (Fig. 4q). Finally, immunoreactivity for GIRK1, GIRK2, and GIRK3 subunits was unaffected by the loss of GIRK4 (Fig. 4f, l, and r). Thus, these data provide further support that GIRK1, GIRK2, and GIRK3 subunits co-assembled to form cerebellar GIRK channels, while GIRK4 contributes very little to channel formation in this brain structure.

GIRK subunits are widely distributed in the cerebellum

We next investigated the regional distribution of all four GIRK subunits in the cerebellum (Fig 4). Using immunohistochemical approaches, by low power observation, we observed that immunolabeling for GIRK1, GIRK2, and GIRK3 subunits were strongest in the granular layer (Fig. 4b, h, and n). The molecular layer was labeled less intensely for GIRK1 and GIRK2 subunits (Fig. 4b and h), while signal was strong for the GIRK3 subunit (Fig. 4n). The PC layer showed weak staining for GIRK1, GIRK2, and GIRK3 subunits, and minimal staining was observed in the white matter (Fig. 4b, h, and n). Finally, using the Tg(Kcnj5-EGFP)49Gsat transgenic mice, which express EGFP under the control of the *Girk4* promoter, we found that the molecular and PC layers were unlabeled, while signal in the granular layer was only observed in a few scattered medium-size neurons, identified as Golgi cells (see below). These observations are largely consistent with previous reports on the limited distribution of GIRK4 mRNA in the cerebellum (Kobayashi *et al.* 1995; Karschin *et al.* 1996; Chen *et al.* 1997).

Cellular and subcellular localization of GIRK subunits

We next used quantitative RT-PCR and immunohistochemical techniques to gain insight into the cellular diversity and subcellular compartments expressing GIRK subunits in the cerebellar cortex, paying special attention to the molecular diversity in the two main cerebellar cell types: granule cells and PCs. Specifically, we used LMD followed by quantitative RT-PCR detection for GIRK subunits and markers of specific cerebellar neuron populations, including GAD65/67 (a marker for basket and stellate cells), calbindin (a marker for PCs), GFAP (a marker for glial cells), and vGluT1 (a marker for granule cells). Observations made are presented below according to cell type.

Granule cells

By quantitative RT-PCR, we observed that granule cells expressed GIRK1, GIRK2, and GIRK3 but not GIRK4 mRNA (Fig. 5a and Table 2). Relative mRNA expression levels were similar for GIRK1 (9.9 ± 0.8, $n = 6$), GIRK2 (15.0 ± 0.7, $n = 7$), and GIRK3 (15.3 ± 0.6, $n = 4$) (Fig. 5a). Using immunohistochemical techniques, we found that granule cells exhibited the most prominent staining for GIRK subunits. Indeed, there was strong staining of the granular layer for all of GIRK1, GIRK2, and GIRK3 subunits, particularly in glomeruli where granule cell dendrites synapse with mossy fiber and Golgi cell terminals

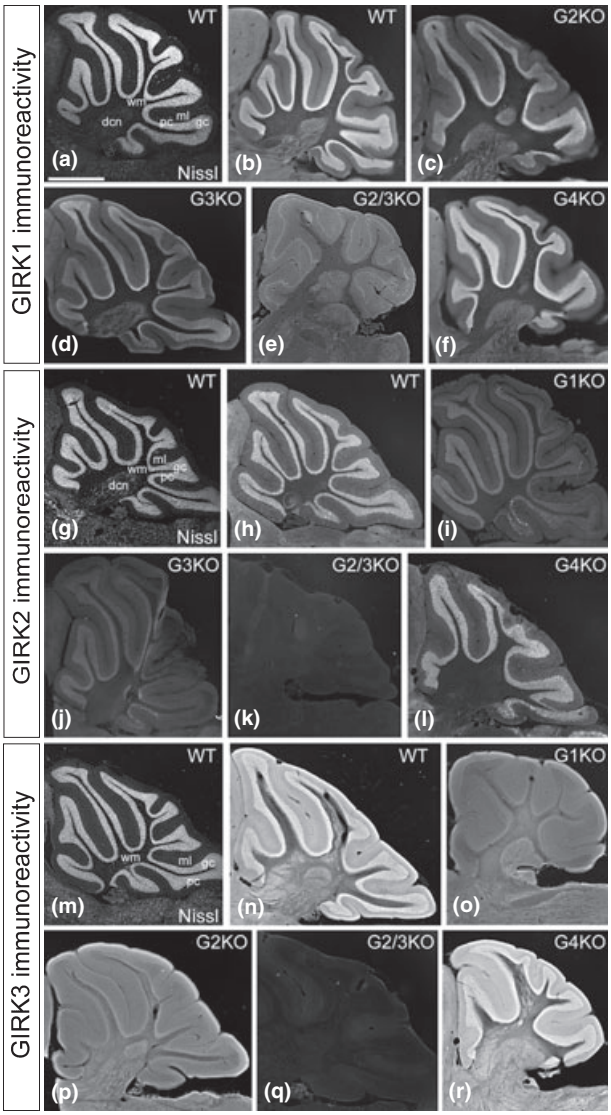

Fig. 4 Regional distribution of GIRK1, GIRK2, and GIRK3 subunits in the cerebellum. Immunohistochemical detection of GIRK1 (a–f), GIRK2 (g–l), and GIRK3 (m–r) in the cerebellum of WT, GIRK1 (G1KO), GIRK2 (G2KO), GIRK3 (G3KO), GIRK2/GIRK3 (G2/3KO), and GIRK4 (G4KO) KO mice is shown. Staining patterns are representative of data obtained from different and complete panels of adult WT and GIRK KO mice. (a, g, and m) Nissl staining in the GIRK1, GIRK2, and GIRK3 cerebella, respectively. (b) GIRK1 immunolabeling in a WT cerebellum, showing high expression in the granule cell layer. (c–e) Residual GIRK1 immunoreactivity in sections from GIRK KO mice. (f) GIRK1 immunolabeling in a section from a GIRK4 KO mouse, showing similar expression pattern than in the WT. (h) GIRK2 immunolabeling in a WT cerebellum, showing high expression in the granule cell layer. (i and j) A significant reduction in GIRK2 immunoreactivity was detected in the cerebellum of G1KO (i) and G3KO (k) mice. (k) GIRK2 immunolabeling was completely absent from the cerebellum of G2/3KO mice. (l) GIRK2 immunolabeling in a section from a GIRK4 KO mouse, showing similar expression pattern than in the WT. (n) GIRK3 immunolabeling in a WT cerebellum, showing high expression in the molecular and granule cell layers. (o and p) A significant reduction in GIRK3 immunoreactivity was detected in the cerebellum of G1KO (o) and G2KO (p) mice. (q) GIRK3 immunolabeling was completely absent from the cerebellum of G2/3KO mice. (r) GIRK3 immunolabeling in a GIRK4 KO mouse, with an expression pattern similar to that seen in WT sections. Abbreviations: ml, molecular layer; pc, Purkinje cell layer; gc, granule cell layer; dcn, deep cerebellar nuclei; wm, white matter. Scale bar: 1 mm.

and in perikaryal rims of granule cells (Fig. 5b–d). In these structures, the three GIRK subunits exhibited strong co-localization (Fig. 5b–d). These staining patterns for GIRK1, GIRK2, and GIRK3 subunits was completely absent in the granule cells of the corresponding GIRK KO mice (Fig. 5e, f, and g).

We next used high-resolution immunoelectron microscopy to determine the subcellular localization of GIRK subunits in granule cells. Using the pre-embedding immunogold method, immunoreactivity for GIRK1, GIRK2, and GIRK3 (Fig. 6) was found primarily at post-synaptic sites along the plasma membrane of granule cell somata (Fig. 6a, h, and l) and dendrites forming glomeruli (Fig. 6b, c, i, j, and m) in WT mice. Labeling was also associated with the ER cisterna of dendritic shafts (22%, 24%, and 27% of all particles examined for GIRK1, GIRK2, and GIRK3, respectively). Of the immunoparticles found in the plasma membrane, most (100% of GIRK1, $n = 892$; 87.2% of GIRK2, $n = 801$; and 81.1% of GIRK3, $n = 1.156$) were found in the post-synaptic compartment. In both GIRK2, and GIRK3 KO mice, the limited labeling for GIRK1 subunit was seen mainly associated with intracellular membranes of granule cell dendritic shafts (75% and 78% of all particles examined, respectively) and very few particles were associated with the plasma membrane (5%) (Fig. 6d and e). In the GIRK2/GIRK3 double KO mice, immunoreactivity for GIRK1 was mainly associated with the ER cisterna (Fig. 6f). Pre-synaptically, immunoparticles for GIRK2 (12.8%) and GIRK3 (18.9%) (Fig. 6i, j, and m), but not for GIRK1 (0%), were also detected along the extrasynaptic membrane of mossy fiber terminals. Labeling for GIRK subunits was never associated with GABAergic axon terminal (Supplementary Fig. S1). Immunoreactivity for GIRK1, GIRK2, and GIRK3 subunits was completely absent in the granule cells of the corresponding GIRK KO mice (Fig. 6g, k, and o).

Purkinje cells

Purkinje cells constitute the sole neurons sending output from the cerebellar cortex and they are heavily excited by granule cell axon terminals. We found that PCs exhibit GIRK1, GIRK2, and GIRK3 mRNAs, but not GIRK4 mRNA (Fig. 7a, Table 2). Furthermore, GIRK3 mRNA was found in all analyzed calbindin-$_{d28k}$- and GAD-positive cell-pools ($n = 8$ of 8), whereas GIRK2 and GIRK1 were expressed only in three and six pools, respectively (Fig. 7a).

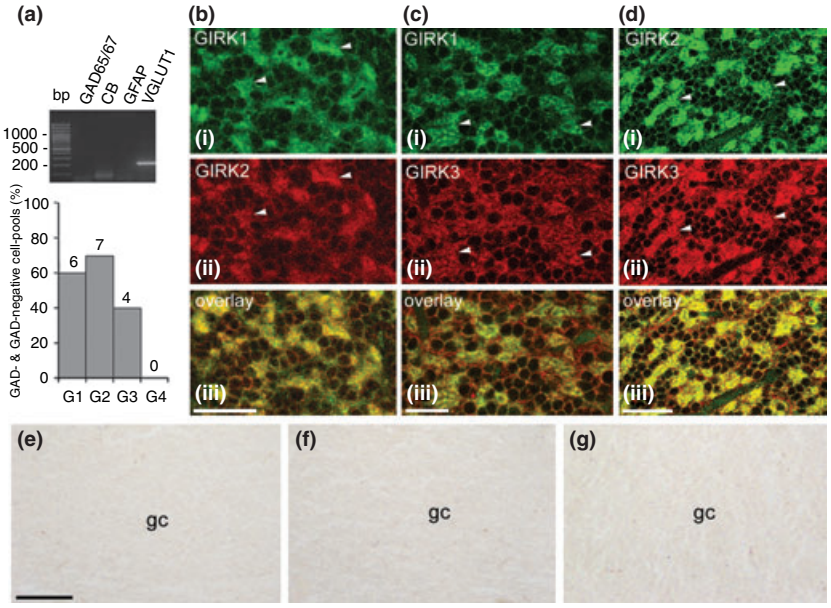

Fig. 5 Distribution of GIRK subunits in granule cells. (a) Qualitative and quantitative RT-PCR analysis of GIRK1-GIRK4 mRNAs in granule cells; upper insert: gel-electrophoresis of qualitative marker PCR, supporting the selectivity of cell-pools. The bar graph displays detection frequencies of GIRK mRNAs, the relative expression levels determined via quantitative SYBR green PCR are given in the Results section. This technique showed that the GIRK1, GIRK2, and GIRK3 subunits, but not the GIRK4 subunit, are present in granule cells. (b–d) The three GIRK subunits are distributed in virtually all granule cells, outlining the soma and strongly staining the glomeruli (arrowheads), with the exception of the mossy fiber axons that were not labeled for GIRK1. Double labeling immunofluorescence showed the co-localization between the GIRK1, GIRK2, and GIRK3 in all granule cells. (e–g) Immunoreactivity for GIRK1, GIRK2, and GIRK3 was completely absent in the granule cells (gc) of the corresponding GIRK KO mice. Scale bars: (b) 30 mm; (c) 20 μm; (d) 33 μm; (e–g) 50 μm.

Table 2 Summary of the distribution of GIRK subunits in cerebellar cell types

Cell type	GIRK1	GIRK2	GIRK3	GIRK4
Stellate cells	–	–	+	–
Basket cells	+	–	+	–
Purkinje cells	+	+	+++	–
Granule cells	+++	+++	+++	–
Golgi cells	–	+++	–	–(+)
Lugaro cells	+	+	+	–
Unipolar brush cells	–	+++	++	–

The intensity of GIRK immunoreactivity was classified as follows: –, little to background level; +, light; ++, moderate; +++, strong. For evaluation of immunosignal intensity, judged by three independent investigators, we used internal standards. As polyclonal antibodies were applied, different affinities and avidities of the respective antibodies could influence the staining intensity. Therefore, this scoring system reflects only relative amounts of immunoreactivity in the different cerebellar cell types rather than a comparison among the three GIRK channel subunits.

Relative mRNA expression levels of GIRK-positive PC pools were 12.4 ± 1.4 for GIRK1 (n = 6), 15.0 ± 4.2 for GIRK2 (n = 3), and 28.0 ± 6.9 for GIRK3 (n = 8), suggesting that GIRK3 is the most abundant GIRK-subunit in PCs (Fig. 7a). Using immunohistochemical methods, GIRK1, GIRK2, and GIRK3 subunits were typically not seen in PC cell bodies but in the neuropil of the molecular layer, making marker co-labeling studies very difficult. Immunoreactivity for GIRK1 and GIRK2 subunits was detected at very low levels throughout the neuropil of the molecular and PC layer (Fig. 7b and d), while immunoreactivity for GIRK3 subunit was relatively strong (Fig. 7e). The presence of GIRK1 expression in PCs was confirmed in sections from GIRK2/GIRK3 double KO mice (Fig. 7c), in which GIRK1 immunoreactivity was concentrated in cellular compartment to likely represent the ER of PCs (Fig. 7l). Immunoreactivity for GIRK1, GIRK2, and GIRK3 subunits was completely absent in the molecular layer and PCs of the corresponding GIRK KO mice (Fig. 7f–h).

Other cell types in the cerebellar cortex

In addition to granule cells and PCs, we also evaluated the expression and distribution of GIRK subunits in several cerebellar cell types including basket cells, stellate cells, Golgi cells, and unipolar brush cells. We identified basket and stellate cells by their distribution in the inner one-third and outer two-thirds of the molecular layer, respectively, and by the expression of GAD65 or GAD67 but not calbindin, GFAP, or vGluT1. Quantitative RT-PCR data suggest that basket cells expressed GIRK1 and GIRK3 mRNAs, but not the GIRK2 or GIRK4 mRNA (Fig. 7i and Table 2). Relative

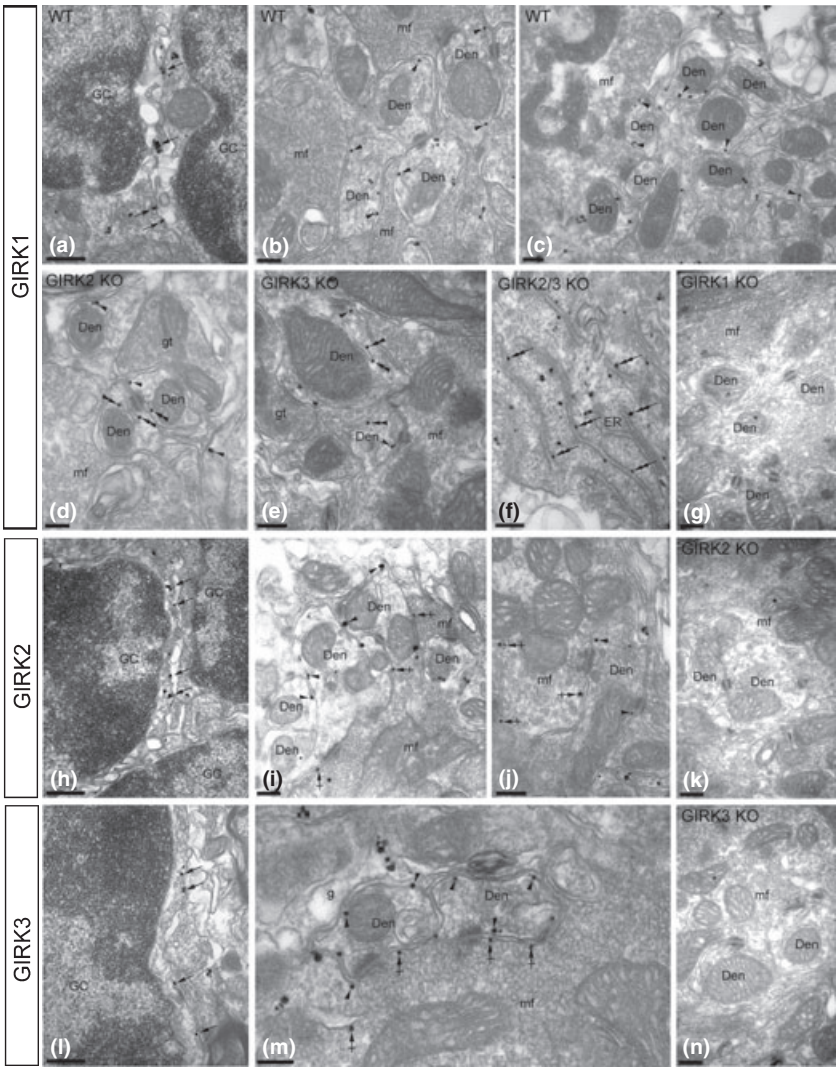

Fig. 6 Subcellular localization of GIRK subunits in granule cells. Electron micrographs show immunolabeling for GIRK1, GIRK2, and GIRK3 in the granule cell layer of WT and GIRK KO mice. (a–c) GIRK1 immunoparticles were observed along the somatic plasma membrane (arrows) and dendrites (Den, arrowheads) of granule cells (GC) from WT mice. GIRK1 was never found at mossy fiber axon terminals (mf). (d–e) In the GIRK2 and GIRK3 KO mice, immunoparticles for GIRK1 were reduced along the plasma membrane (arrowheads) of dendrites (Den) and primarily found associated with intracellular membranes (double arrowheads). (f) In the GIRK2/GIRK3 double KO mice, GIRK1 labeling was found associated with the endoplasmic reticulum (ER) of granule cells (double arrows). (g) Immunoreactivity for GIRK1 was completely absent in the GIRK1 KO mice. (h–j) GIRK2 immunoparticles were observed along the somatic plasma membrane (arrows) and dendrites (Den, arrowheads) of granule cells (GC), as well as at pre-synaptic sites along the plasma membrane (crossed arrows) of mossy fiber axon terminals (mf). (k) Immunoreactivity for GIRK2 was completely absent in the GIRK2 KO mice. (l–m) Immunoparticles for GIRK3 were found along the somatic plasma membrane (arrows) and dendrites (Den, arrowheads) of granule cells (GC), as well as on glial (g) cells surrounding the glomeruli. Pre-synaptically, GIRK3 immunoparticles were frequently observed along the plasma membrane (crossed arrows) of mossy fiber axon terminals (mf). (n) Immunoreactivity for GIRK3 was completely absent in the GIRK3 KO mice. Scale bars: (a, h, l, and f) 0.1 μm; (b–e, g, i–k, and m–o) 0.2 μm.

mRNA expression levels of GIRK-positive cell-pools were 7.6 ± 5.8 for GIRK1 (n = 4) and 12.3 ± 2.9 for GIRK3 (n = 6) in basket cells (Fig. 7i). In stellate cells, quantitative data suggested very low levels of GIRK3 mRNA (3.1 ± 1.0, n = 6) (Fig. 7j and Table 2). Using immunohistochemical methods, the expression of GIRK subunits in basket and stellate cells was found to be very low in WT mice, bordering on the detection threshold of the technique. Perikaryal accumulation of GIRK1 in sections from GIRK2/GIRK3 double KO suggested that GIRK1 is normally found in basket cells (Fig. 7k and l) but not in stellate cells (Fig. 7m).

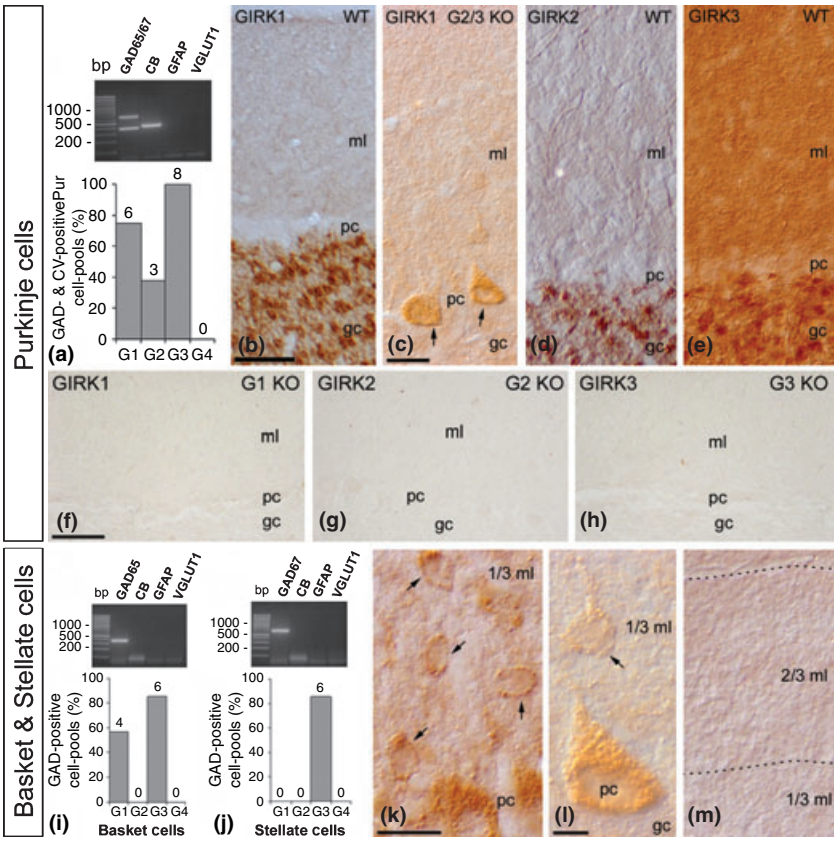

Fig. 7 Distribution localization of GIRK subunits in Purkinje cells, basket cells, and stellate cells. (a) RT-PCR analysis of GIRK1–GIRK4 mRNAs in selective pools of Purkinje cells; upper insert: gel-electrophoresis of qualitative marker PCR, supporting the selectivity of cell-pools. The bar graph displays detection frequencies of GIRK mRNAs, the relative expression levels determined via quantitative SYBR green PCR are given in the Results section. (b–e) The presence of the three GIRK subunits in Purkinje cells was corroborated using immunohistochemical techniques. Because of the low expression of GIRK1 in the Purkinje cell layer (pc) and molecular layer (ml) of WT cerebella (panel b), the presence of this subunit in Purkinje cells (arrows) was validated by observations made in parallel using sections from G2/3 double KO mice (panel c). In these sections GIRK1 labeling was concentrated in the endoplasmic reticulum (see panel l), consistent with its inability to traffic to the cell membrane in the absence of other GIRK subunits. Immunoreactivity for GIRK2 in Purkinje cells was low, but moderate to strong for GIRK3. (f–h) At light microscopic level, immunoreactivity for GIRK1, GIRK2, and GIRK3 was completely absent in the corresponding GIRK KO mice. (i and j) Qualitative and quantitative RT-PCR analysis of GIRK1–GIRK4 mRNAs in basket and stellate cells; upper insert: gel-electrophoresis of qualitative marker PCR, supporting the selectivity of cell-pools. The bar graph displays detection frequencies of GIRK mRNAs, the relative expression levels determined via quantitative SYBR green PCR are given in the Results section. (k–m) Parallel comparisons of sections from WT and GIRK2/GIRK3 double KO mice permitted the detection of GIRK1 in basket cells (arrows), located in the inner one third of the molecular layer (1/3 ml), *but not* stellate cells, which are located in the outer two third of the molecular layer (2/3 ml). gc, granule cell layer. Scale bars: (k) 10 μm; (b–e, l, and m) 40 μm; (f–h) 50 μm.

Golgi cells are located in the granular layer and extend their dendrites throughout the molecular layer. As their soma is fully surrounded by granule cells, it was difficult to isolate them using UV-laser microdissection, as we could not rule out some contamination. Using immunohistochemical techniques, we found that most Golgi cells only expressed GIRK2 subunit (Fig. 8a and Table 2, and also see Fig. 7b–e). This finding was confirmed using double-labeling experiments with the metabotropic glutamate receptor subtype $mGlu_{2/3}$, a specific marker of Golgi cells (Fig. 8b). Furthermore, using the Tg(Kcnj5-EGFP)49Gsat transgenic mice, which express EGFP under the control of the *Girk4* promoter, we found that a small population of Golgi cells also express GIRK4, always together with GIRK2 (Fig. 8c and Table 2). Using vesicular GABA transporter, a presynaptic marker for Golgi cell axons in the granular layer, however, we further showed that only very few Golgi cells expressed EGFP (Fig. 8d). We conclude that Golgi cells express GIRK2, with a small subset also expressing GIRK4.

Finally, unipolar brush cells are located primarily in the granular layer of the vestibule-cerebellum, in lobule IX and X, and are unique medium-size interneurons with a brush-like dendrite structure. We could not perform RT-PCR on this cell type because they are surrounded by granule cells

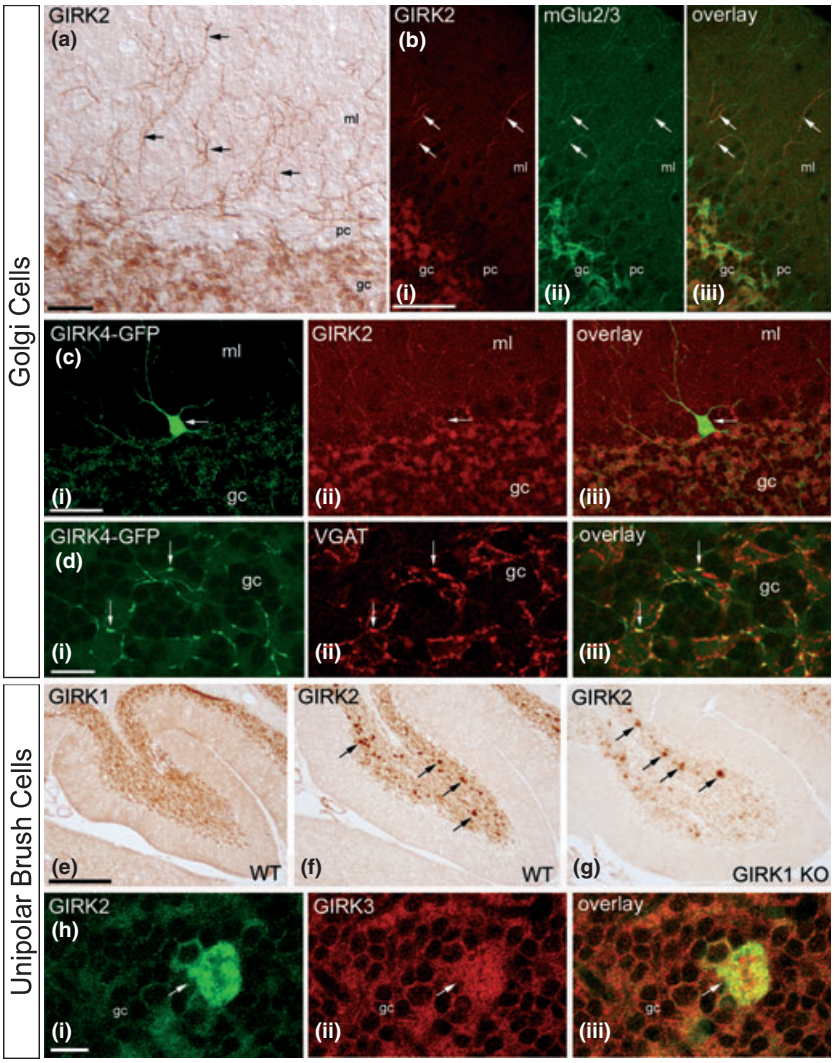

Fig. 8 Distribution of GIRK subunits in Golgi cells and unipolar brush cells. (a and b) Dendrites of Golgi cells running through the molecular layer (ml) were strongly immunoreactive for GIRK2 (arrows). Double immunofluorescence showed that GIRK2-immunoreactive dendrites co-localized (arrows) with mGlu2/3, a marker of Golgi cells. (c), Using Tg(Kcnj5-EGFP)49Gsat transgenic mice, we detected a subset of Golgi cells that likely express GIRK4, and that always co-localized with GIRK2 (arrows). (d) Double immunofluorescence of granular layer showing that all EGFP-positive axon terminals express the GABAergic marker VGAT (arrows). (e–g) Distribution of GIRK subunits in unipolar brush cells (arrows) of lobule X. GIRK1 immunoreactivity was not detected in these cells (panel e), despite the relatively high level of expression of GIRK2 (arrows in panel f). Immunoreactivity for GIRK2 was not affected by the loss of GIRK1 (arrows in panel g), suggesting that GIRK1 and GIRK2 do not form heteromeric channels in unipolar brush cells. (h) Double immunofluorescence of lobule X granular layer showing that unipolar brush cells express both GIRK2 and GIRK3. Scale bars: (a) 40 μm; (b) 75 μm; (c) 48 μm; (d) 10 μm; (e–h) 20 μm; (g) 11 μm.

making difficult its isolation using UV-laser microdissection. Using immunohistochemical techniques, GIRK1 was not detected in unipolar brush cells (Fig. 8e), though labeling was quite strong for GIRK2 subunit (Fig. 8f). This finding was supported by the fact that immunoreactivity for GIRK2 subunit in unipolar brush cells was not affected by the loss of GIRK1 (Fig. 8g). Using double labeling immunofluorescence, we found that virtually all unipolar brush cells immunoreactive for GIRK2 also expressed GIRK3 (Fig. 8h and Table 2).

Discussion

G protein-gated inwardly rectifying K^+ channels play an important role in controlling neuronal excitability by generating slow inhibitory potentials following the activation of G protein-coupled receptors. In the present study, we examined how GIRK channel subunits are expressed and distributed in cerebellar neurons by biochemical and morphological techniques. We have demonstrated for the first time clear co-assemblies among GIRK1, GIRK2, and GIRK3 in the cerebellum, and that major cerebellar neuron populations, such as PCs and granule cells, express all three GIRK subunits, while we see an intriguing variety of expression patterns among the lesser represented cerebellar populations. Our findings demonstrate that GIRK subunits are distributed in a cell type-dependent manner, supporting the existence of significant molecular and cellular diversity in the cerebellar GIRK channel population.

Cerebellar GIRK channels are co-assembled from GIRK1–3 subunits

Previous co-immunoprecipitation experiments have suggested that a significant fraction of neuronal GIRK channels are heteromultimers composed of GIRK1 and GIRK2 (Kofuji *et al.* 1995, 1996; Lesage *et al.* 1995; Liao *et al.* 1996; Slesinger *et al.* 1996). Heteromeric GIRK2/GIRK3 complexes have also been shown to exist in the brain (Jelacic

et al. 2000). In the present study, co-immunoprecipitation experiments revealed that GIRK1, GIRK2, and GIRK3 antibodies each co-immunoprecipitated the other two subunits in solubilized cerebellar membranes. Moreover, we observed significant alterations in expression levels and patterns of GIRK1, GIRK2, and GIRK3 subunits in tissue from GIRK KO mice. The dramatic reduction of GIRK1 staining in GIRK2 KO mice is consistent with previous reports (Liao *et al.* 1996; Signorini *et al.* 1997; Torrecilla *et al.* 2002; Koyrakh *et al.* 2005). We further found that the level of GIRK2 subunit was decreased in GIRK1 and GIRK3 KO mice, and that of GIRK3 subunit was decreased in GIRK1 and GIRK2 KO mice. In contrast, no apparent changes were seen for immunohistochemical staining of GIRK1, GIRK2, and GIRK3 subunits in the cerebellum of GIRK4 KO mice. This is most likely because of the lack or restricted cellular expression of GIRK4 in the cerebellum. Indeed, this contention is supported by *in situ* hybridization (Wickman *et al.* 2000) and cell-type specific quantitative RT-PCR, and the dearth of labeling of cerebellar cell types seen in the Tg(Kcnj5-EGFP)49Gsat transgenic animal. Altogether, our results indicate that major cerebellar GIRK channels are formed by co-assembly among GIRK1, GIRK2, and GIRK3 subunits.

Molecular and cellular diversity of cerebellar GIRK channels

As the subunit composition may determine the subcellular distribution and/or functional properties of the GIRK channel, high-resolution information on cellular and subcellular distribution of individual GIRK subunits is essential. Here, based upon the overlapping but distinct expression patterns for GIRK subunits in the cerebellum, and with the assumption that subunits expressed in a given cell-type co-assembled to form channel complexes, we infer the existence of at least six distinct GIRK channel subtypes in the various cell types of the mouse cerebellum: GIRK1/GIRK2/GIRK3 heteromultimers in Purkinje and granule cells; GIRK2 homomultimers and GIRK2/GIRK4 heteromultimers in Golgi cells; GIRK3 homomultimers in stellate cells; GIRK1/GIRK3 heteromultimers in basket cells; and GIRK2/GIRK3 heteromultimers in unipolar brush cells.

Native GIRK channels are thought to exist in the brain as homomeric channels composed of one subunit type or as heteromeric complexes of two or more subunit types or isoforms (Kobayashi *et al.* 1995; Karschin *et al.* 1996; Chen *et al.* 1997). GIRK1 alone does not form functional homomeric channels and requires co-expression with other subunits to achieve membrane localization (Duprat *et al.* 1995; Kofuji *et al.* 1995; Krapivinsky *et al.* 1995b; Hedin *et al.* 1996; Kennedy *et al.* 1999; Ma *et al.* 2002). GIRK2, however, can form functional homomeric as well as heteromeric channels in the brain. For instance, homomeric GIRK2 channels are present in dopaminergic neurons of the substantia nigra (Liss *et al.* 1999; Jelacic *et al.* 2000; Koyrakh *et al.* 2005), although strictly speaking they are heteromeric channels formed by the combination of GIRK2A and GIRK2C isoforms (Inanobe *et al.* 1999b), while heteromeric GIRK1/GIRK2 channels, widely considered the prototypical GIRK channel in the CNS, have been described in pyramidal cells of the hippocampus (Liao *et al.* 1996; Koyrakh *et al.* 2005).

Many studies have highlighted an essential role of GIRK2 in the formation of functional GIRK channels. Indeed, baclofen-evoked GIRK channel-mediated currents were significantly reduced in cerebellar neurons from GIRK2 KO and *weaver* mice (Slesinger *et al.* 1997). Consistent with the observation, we found GIRK2 expression in many cerebellar neurons, i.e. PCs, granule cells, Golgi cells, and unipolar brush cells. However, we also identified some cells that lack the GIRK2 subunit. In these cells, GIRK3 is commonly expressed together with (basket cells) or without (stellate cells) GIRK1. Furthermore, quantitative RT-PCR data and immunohistochemistry suggest that GIRK3 is the most prominent subunit in PCs.

The contribution of GIRK3 to neuronal GIRK channel formation remains controversial. Although it has been proposed that GIRK3 is involved in directing functional GIRK channels toward lyzosomal degradation (Ma *et al.* 2002), several studies have suggested that GIRK3 forms functional channels (Jelacic *et al.* 1999, 2000; Torrecilla *et al.* 2002; Koyrakh *et al.* 2005). In this regard, our finding that the level of heavily glycosylated (membrane-associated) GIRK1 was significantly lower in the cerebellum of GIRK2/GIRK3 double KO mice when compared with GIRK2 single KO mice is of great interest. This raises the possibility that a significant proportion of cerebellar GIRK channels exists as GIRK1/GIRK3 heteromeric channels. In future studies, it will be important to address whether GIRK1/GIRK3 heteromeric and GIRK3 homomeric channels are functional by examining GIRK currents in cerebellar neurons from GIRK2 KO mice.

Another noteworthy observation from this study was that all neuronal GIRK subunits were expressed in major cerebellar neurons (PCs and granule cells). In these cell types, the subcellular localization of the three GIRK subunits was almost identical. In the granule cells, the GIRK subunits were found in the same portion of plasma membrane. These expression and localization patterns suggest that a variety of heteromeric, as well as homomeric channels, could be generated in these neurons. It is also possible that the major form of GIRK channels in PCs and granule cells might be a complex containing all three GIRK1/GIRK2/GIRK3 subunits. We cannot exclude the possibility, however, that differential sorting mechanisms preclude the formation of certain heteromultimeric channel complexes in a particular cell type.

GIRK channels are localized at post- and pre-synaptic sites in the cerebellum

Neuronal GIRK channel mediate the post-synaptic inhibitory effects of many neurotransmitters and drugs of abuse that

target Gi/o-coupled receptors (Signorini *et al.* 1997; Lüscher and Ungless 2006). Here, we offer direct evidence that GIRK channel subunits in the cerebellum are found predominantly at post-synaptic sites (i.e. somatic and dendritic compartments of granule cells), which is consistent with previous studies in the hippocampus, neocortex, and spinal cord (Ponce *et al.* 1996; Drake *et al.* 1997; Lüscher *et al.* 1997; Takigawa and Alzheimer 1999; Chen and Johnston 2005; Koyrakh *et al.* 2005; Marker *et al.* 2005; Kulik *et al.* 2006). We did, however, find some specific pre-synaptic labeling for GIRK subunits in glutamatergic axon terminals in the cerebellum, including mossy fibers, but never associated with GABAergic terminals. Pre-synaptic labeling for GIRK subunits has been shown in other brain regions, including the hippocampus, substantia nigra, hypothalamus, and spinal cord (Morishige *et al.* 1996; Ponce *et al.* 1996; Koyrakh *et al.* 2005; Marker *et al.* 2005). However, functional studies involving GIRK2 KO and GIRK2/GIRK3 double KO mice have failed to support a measurable contribution of GIRK channels to the pre-synaptic inhibitory effects of many neurotransmitters (Lüscher *et al.* 1997). Pre-synaptic inhibition is thought to result primarily from G protein-dependent direct suppression of voltage-gated Ca^{2+} channel activity (Dolphin 2003). The possible role of neuronal GIRK channels at axonal termini warrants additional attention.

Physiological implications of GIRK channels in cerebellar cells

Activation of GIRK channels causes membrane hyperpolarization (Lüscher *et al.* 1997) and, as such, these channels are important determinants of cell excitability. In the cerebellum, electrophysiological studies have demonstrated the presence of GIRK currents in several neurons, including PCs and granule cells (Slesinger *et al.* 1997; Han *et al.* 2003; Tabata *et al.* 2005). However, the functional implications of GIRK subunit composition are poorly understood. It has been established that GIRK1 can assemble with any of the three other GIRK subunits to form heterotetrameric channels with virtually identical electrophysiological properties and Gβγ sensitivities (Jelacic *et al.* 1999). In contrast, homomeric GIRK channels have different electrophysiological properties (Krapivinsky *et al.* 1995a; Wischmeyer *et al.* 1997; Jelacic *et al.* 1999). In addition, heteromeric GIRK2/GIRK3 channels have slightly smaller single channel conductance and less sensitivity to activation by Gβγ than GIRK1-containing channels (Jelacic *et al.* 2000). Therefore, our findings suggest that neuronal GIRK channels present in different cerebellar neuron types may exhibit with distinct electrophysiological properties, Gβγ sensitivity and association with specific neurotransmitter receptors. Because a variety of G protein-coupled inhibitory receptors, including metabotropic GABA receptors, metabotropic glutamate receptors, adenosine A_1 receptors, and serotonergic receptors activate GIRK channels in the cerebellum (North 1989), further studies on functional properties are required to elucidate their physiological roles in the control of cerebellar functions.

Acknowledgements

The authors would like to thank Dr Toshihide Tabata, Professor Masanobu Kano, Dr Sergi Ferre, and Dr John P. Adelman for their comments on the manuscript. We also would like to thank to Mr José Julio Cabanes and Ms María José Simarro for the excellent technical assistance. FC is currently holding a Ramón y Cajal research contract signed with the Spanish Ministry of Education and Science. This work was supported by grants from the Spanish Ministry of Education and Science (BFU-2006-01896 to RL and SAF2005-00903 to FC), from the NIH (MH61933 and DA011806 to KW and MH078291 to JC) and from the Hertie-foundation and the NGFN-II to BL.

Supplementary material

The following supplementary material is available for this article online:

Fig. S1 Absence of GIRK expression in GABAergic terminals.

This material is available as part of the online article from http://www.blackwell-synergy.com.

Please note: Blackwell Publishing are not responsible for the content or functionality of any supplementary materials supplied by the authors. Any queries (other than missing material) should be directed to the corresponding author for the article.

References

Bettahi I., Marker C. L., Roman M. I. and Wickman K. (2002) Contribution of the Kir3.1 subunit to the muscarinic-gated atrial potassium channel IKACh. *J. Biol. Chem.* **277**, 48282–48288.

Burgueno J., Blake D. J., Benson M. A. *et al.* (2003) The adenosine A2A receptor interacts with the actin-binding protein alpha-actinin. *J. Biol. Chem.* **278**, 37545–37552.

Chen X. and Johnston D. (2005) Constitutively active G-protein-gated inwardly rectifying K+ channels in dendrites of hippocampal CA1 pyramidal neurons. *J. Neurosci.* **25**, 3787–3792.

Chen S. C., Ehrhard P., Goldowitz D. and Smeyne R. J. (1997) Developmental expression of the GIRK family of inward rectifying potassium channels: implications for abnormalities in the *weaver* mutant mouse. *Brain Res.* **778**, 251–264.

Ciruela F., Escriche M., Burgueno J. *et al.* (2001) Metabotropic glutamate 1alpha and adenosine A1 receptors assemble into functionally interacting complexes. *J. Biol. Chem.* **276**, 18345–18351.

Cruz H. G., Ivanova T., Lunn M. L., Stoffel M., Slesinger P. A. and Luscher C. (2004) Bi-directional effects of GABA(B) receptor agonists on the mesolimbic dopamine system. *Nat. Neurosci.* **7**, 153–159.

Dolphin A. C. (2003) G protein modulation of voltage-gated calcium channels. *Pharmacol. Rev.* **55**, 607–627.

Drake C. T., Bausch S. B., Milner T. A. and Chavkin C. (1997) GIRK1 immunoreactivity is present predominantly in dendrites, dendritic spines, and somata in the CA1 region of the hippocampus. *Proc. Natl Acad. Sci. USA* **94**, 1007–1012.

Duprat F., Lesage F., Guillemare E., Fink M., Hugnot J.-P., Bigay J., Lazdunski M., Romey G. and Barhanin J. (1995) Heterologous multimeric assembly is essential for K+ channel activity of neu-

ronal and cardiac G-protein activated inward rectifiers. *Biochem. Biophys. Res. Commun.* **212**, 657–663.

Fukudome Y., Ohno-Shosaku T., Matsui M., Omori Y., Fukaya M., Taketo M., Watanabe M., Manabe M. and Kano M. (2004) Two distinct classes of muscarinic action on hippoccampal inhibitory synapses: M2-mediated direct suppression and M1/M3-mediated indirect suppression through endocannabinoid signaling. *Eur. J. Neurosci.* **19**, 2682–2692.

Han J., Kang D. and Kim D. (2003) Properties and modulation of the G protein-coupled K+ channel in rat cerebellar granule neurons: ATP versus phosphatidylinositol 4,5-bisphosphate. *J. Physiol.* **550**, 693–706.

Hedin K. E., Lim N. F. and Clapham D. E. (1996) Cloning of a *Xenopus laevis* inwardly rectifying K+ channel subunit that permits GIRK1 expression of IKACh currents in oocytes. *Neuron* **16**, 423–429.

Inanobe A., Horio Y., Fujita A., Tanemoto M., Hibino H., Inageda K. and Kurachi Y.(1999a) Molecular cloning and characterization of a novel splicing variant of the Kir3.2 subunit predominantly expressed in mouse testis. *J. Physiol.* **15**(521 Pt. 1), 19–30.

Inanobe A., Yoshimoto Y., Horio Y. *et al.* (1999b) Characterization of G-protein-gated K+ channels composed of Kir3.2 subunits in dopaminergic neurons of the substantia nigra. *J. Neurosci.* **19**, 1006–1017.

Jelacic T. M., Sims S. M. and Clapham D. E. (1999) Functional expression and characterization of G-protein-gated inwardly rectifying K+ channels containing GIRK3. *J. Membr. Biol.* **169**, 123–129.

Jelacic T. M., Kennedy M. E., Wickman K. and Clapham D. E. (2000) Functional and biochemical evidence for G-protein-gated inwardly rectifying K+ (GIRK) channels composed of GIRK2 and GIRK3. *J. Biol. Chem.* **275**, 36211–36216.

Karschin C., Dissmann E., Stuhmer W. and Karschin A. (1996) IRK(1–3) and GIRK(1–4) inwardly rectifying K+ channel mRNAs are differentially expressed in the adult rat brain. *J. Neurosci.* **16**, 3559–3570.

Kennedy M. E., Nemec J. and Clapham D. E. (1996) Localization and interaction of epitope-tagged GIRK1 and CIR inward rectifier K+ channel subunits. *Neuropharmacology* **35**, 831–839.

Kennedy M. E., Nemec J., Corey S., Wickman K. and Clapham D. E. (1999) GIRK4 confers appropriate processing and cell surface localization to G-protein gated potassium channels. *J. Biol. Chem.* **274**, 2571–2582.

Kobayashi T., Ikeda K., Ichikawa T., Abe S., Togashi S. and Kumanishi T. (1995) Molecular cloning of a mouse G-protein-activated K+ channel (mGIRK1) and distinct distributions of three GIRK (GIRK1, 2 and 3) mRNAs in mouse brain. *Biochem. Biophys. Res. Commun.* **208**, 1166–1173.

Kofuji P., Davidson N. and Lester H. A. (1995) Evidence that neuronal G-protein-gated inwardly rectifying K+ channels are activated by G beta gamma subunits and function as heteromultimers. *Proc. Natl Acad. Sci. USA* **92**, 6542–6546.

Kofuji P., Hofer M., Millen K. J., Millonig J. H., Davidson N., Lester H. A. and Hatten M. E. (1996) Functional analysis of the weaver mutant GIRK2 K+ channel and rescue of weaver granule cells. *Neuron* **16**, 941–952.

Koyrakh L., Luján R., Colon J., Karschin C., Kurachi Y., Karschin A. and Wickman K. (2005) Molecular and cellular diversity of neuronal G-protein-gated potassium channels. *J. Neurosci.* **25**, 11468–11478.

Krapivinsky G., Gordon E. A., Wickman K., Velimirovic B., Krapivinsky L. and Clapham D. E. (1995a) The G-protein-gated atrial K+ channel IKACh is a heteromultimer of two inwardly rectifying K+-channel proteins. *Nature* **374**, 135–141.

Krapivinsky G., Krapivinsky L., Velimirovic B., Wickman K., Navarro B. and Clapham D. E. (1995b) The cardiac inward rectifier K+ channel subunit, CIR, does not comprise the ATP-sensitiveK+ channel, IKATP. *J. Biol. Chem.* **270**, 28777–28779.

Kulik A., Vida I., Fukazawa Y. *et al.* (2006) Compartment-dependent colocalization of Kir3.2-containing K+ channels and $GABA_B$ receptors in hippocampal pyramidal cells. *J. Neurosci.* **26**, 4289–4297.

Lesage F., Guillemare E., Fink M., Duprat F., Heurteaux C., Fosset M., Romey G., Barhanin J. and Lazdunski M. (1995) Molecular properties of neuronal G-protein-activated inwardly rectifying K+ channels. *J. Biol. Chem.* **270**, 28660–28667.

Liao Y. J., Jan Y. N. and Jan L. Y. (1996) Heteromultimerization of G-protein-gated inwardly rectifying K+ channel proteins GIRK1 and GIRK2 and their altered expression in *weaver* brain. *J. Neurosci.* **16**, 7137–7150.

Liss B. (2002) Improved quantitative real-time RT-PCR for expression profiling of individual cells. *Nucleic Acids Res.* **30**, e89.

Liss B., Neu A. and Roeper J. (1999) The weaver mouse gain-of-function phenotype of dopaminergic midbrain neurons is determined by coactivation of wvGirk2 and K-ATP channels. *J. Neurosci.* **19**, 8839–8848.

Liss B., Haeckel O., Wildmann J., Miki T., Seino S. and Roeper J. (2005) K-ATP channels promote the differential degeneration of dopaminergic midbrain neurons. *Nat. Neurosci.* **8**, 1742–1751.

López-Bendito G., Shigemoto R., Kulik A., Paulsen O., Fairén A. and Luján R. (2002) Expression and distribution of metabotropic GABA receptor subtypes GABABR1 and GABABR2 during rat neocortical development. *Eur. J. Neurosci.* **15**, 1766–1778.

Luján R., Nusser Z., Roberts J. D., Shigemoto R. and Somogyi P. (1996) Perisynaptic location of metabotropic glutamate receptors mGluR1 and mGluR5 on dendrites and dendritic spines in the rat hippocampus. *Eur. J. Neurosci.* **8**, 1488–1500.

Lüscher C. and Ungless M. A. (2006) The mechanistic classification of addictive drugs. *PLoS Med.* **3**, e437.

Lüscher C., Jan L. Y., Stoffel M., Malenka R. C. and Nicoll R. A. (1997) G protein-coupled inwardly rectifying K+ channels (GIRKs) mediate postsynaptic but not presynaptic transmitter actions in hippocampal neurons. *Neuron* **19**, 687–695.

Ma D., Zerangue N., Raab-Graham K., Fried S. R., Jan Y. N. and Jan L. Y. (2002) Diverse trafficking patterns due to multiple traffic motifs in G protein-activated inwardly rectifying potassium channels from brain and heart. *Neuron* **33**, 715–729.

Marker C. L., Cintora S. C., Roman M. I., Stoffel M. and Wickman K. (2002) Hyperalgesia and blunted morphine analgesia in G protein-gated potassium channel subunit knockout mice. *NeuroReport* **13**, 2509–2513.

Marker C., Luján R., Loh H. and Wickman K. (2005) Spinal G protein-gated potassium channels contribute in a dose-dependent manner to the analgesic effect of mu and delta but not kappa opioids. *J. Neurosci.* **25**, 3551–3559.

Morishige K. I., Inanobe A., Takahashi N., Yoshimoto Y., Kurachi H., Miyake A., Tokunaga Y., Maeda T. and Kurachi Y. (1996) G protein-gated K+ channel (GIRK1) protein is expressed presynaptically in the paraventricular nucleus of the hypothalamus. *Biochem. Biophys. Res. Commun.* **220**, 300–305.

Murer G., Adelbrecht C., Lauritzen I., Lesage F., Lazdunski M., Agid Y. and Raisman-Vozari R. (1997) An immunocytochemical study on the distribution of two G-protein-gated inward rectifier potassium channels (GIRK2 and GIRK4) in the adult rat brain. *Neuroscience* **80**, 345–357.

Nakamura M., Sato K., Fukaya M., Araishi K., Aiba A., Kano M. and Watanabe M. (2004) Signaling complex formation of phospholipase Cbeta4 with metabotropic glutamate receptor type 1alpha and 1,4,5-trisphosphate receptor at the perisynapse and endoplasmic reticulum in the mouse brain. *Eur. J. Neurosci.* **20**, 292929–292944.

North A. (1989) Drug receptors and the inhibition of nerve cells. *Br. J. Pharmacol.* **98**, 13–28.

Ponce A., Bueno E., Kentros C. *et al.* (1996) G-protein-gated inward rectifier K+ channel proteins (GIRK1) are present in the soma and dendrites as well as in nerve terminals of specific neurons in the brain. *J. Neurosci.* **16**, 1990–2001.

Signorini S., Liao Y. J., Duncan S. A., Jan L. Y. and Stoffel M. (1997) Normal cerebellar development but susceptibility to seizures in mice lacking G protein-coupled, inwardly rectifying K+ channel GIRK2. *Proc. Natl Acad. Sci. USA* **94**, 923–927.

Slesinger P. A., Patil N., Liao J., Jan Y. N., Jan L. Y. and Cox D. R. (1996) Functional effects of the mouse *weaver* mutation on G protein-gated inwardly rectifying K+ channels. *Neuron* **16**, 321–331.

Slesinger P., Stoffel M., Jan Y. and Jan L. (1997) Defective g-aminobutyric acid type B receptor-activated inwardly rectifying K+ currents in cerebellar granule cells isolated from *weaver* and *Girk2* null mutant mice. *Proc. Natl Acad. Sci. USA* **94**, 12210–12217.

Tabata T., Haruki S., Nakayama H. and Kano M. (2005) GABAergic activation of an inwardly rectifying K+ current in mouse cerebellar Purkinje cells. *J. Physiol.* **563**, 443–457.

Takigawa T. and Alzheimer C. (1999) G protein-activated inwardly rectifying K+ (GIRK) currents in dendrites of rat neocortical pyramidal cells. *J. Physiol. (Lond.)* **517**, 385–390.

Torrecilla M., Marker C. L., Cintora S. C., Stoffel M., Williams J. T. and Wickman K. (2002) G-protein-gated potassium channels containing Kir3.2 and Kir3.3 subunits mediate the acute inhibitory effects of opioids on locus ceruleus neurons. *J. Neurosci.* **22**, 4328–4334.

Wei J., Hodes M. E., Piva R., Feng Y., Wang Y., Ghetti B. and Dlouhy S. R. (1998) Characterization of murine Girk2 transcript isoforms: structure and differential expression. *Genomics* **51**, 379–390.

Wickman K., Nemec J., Gendler S. J. and Clapham D. E. (1998) Abnormal heart rate regulation in GIRK4 knockout mice. *Neuron* **20**, 103–114.

Wickman K., Karschin C., Karschin A., Picciotto M. R. and Clapham D. E. (2000) Brain localization and behavioral impact of the G-protein-gated K+ channel subunit GIRK4. *J. Neurosci.* **20**, 5608–5615.

Wischmeyer E., Doring F., Wischmeyer E., Spauschus A., Thomzig A., Veh R. and Karschin A. (1997) Subunit interactions in the assembly of neuronal Kir3.0 inwardly rectifying K+ channels. *Mol. Cell. Neurosci.* **9**, 194–206.

